HHS Public Access

Author manuscript

Vaccine. Author manuscript; available in PMC 2022 April 28.

Published in final edited form as:

Vaccine. 2021 April 28; 39(18): 2526–2536. doi:10.1016/j.vaccine.2021.03.075.

Lack of Neonatal Fc Receptor does not Diminish the Efficacy of the HSV-1 0ΔNLS Vaccine Against Ocular HSV-1 Challenge

Daniel J.J. Carr[a,b,*], **Amanda N. Berube**[a], **Adrian Filiberti**[a], **Grzegorz B. Gmyrek**[a]

[a]Department of Ophthalmology, University of Oklahoma Health Sciences Center, Oklahoma City, OK 73104, USA

[b]Department of Microbiology and Immunology, University of Oklahoma Health Sciences Center, Oklahoma City, OK 73104, USA

Abstract

The neonatal Fc receptor (FcRn) is constitutively expressed in the cornea and is up-regulated in response to herpes simplex virus type 1 (HSV-1). Previously, we found targeting cornea FcRn expression by small interfering RNA-mediated knockdown reduced the local efficacy of HSV-1 0ΔNLS vaccinated C57BL/6 mice against ocular challenge with HSV-1. The current study was undertaken to evaluate the HSV-1 0ΔNLS vaccine efficacy in FcRn deficient (FcRn KO) mice challenged with HSV-1. Whereas there was little neutralizing antibody detected in the serum of HSV-1 0ΔNLS vaccinated FcRn KO mice, these mice exhibited the same degree of protection against ocular challenge with HSV-1 as wild type (WT) C57BL/6 mice as measured by cumulative survival, infectious virus shed or retained in tissue, and corneal pathology including opacity and neovascularization. Mock-vaccinated FcRn KO mice were found to be more sensitive to ocular HSV-1 infection compared to mock-vaccinated (WT) mice in terms of cumulative survival and virus shedding. In addition, the FcRn KO mice generated significantly fewer effector ($CD3^+CD44^+CD62L^-$) and central ($CD3^+CD44^+CD62L^+$) memory $CD8^+$ T cells compared to the WT mice 7 days post infection. Collectively, mock-vaccinated FcRn KO mice are susceptible to ocular HSV-1 infection but HSV-1 0ΔNLS vaccinated FcRn KO mice are resistant suggesting that in addition to the FcRn, other pathways are involved in mediating the protective effect of the HSV-1 0ΔNLS vaccine against subsequent HSV-1 challenge.

*Corresponding author at: Department of Ophthalmology, University of Oklahoma Health Sciences Center, 608 Stanton L. Young Blvd., DMEI #415A, Oklahoma City, OK. 73104, USA, dan-carr@ouhsc.edu.

Declaration of competing interest

DJJC is a member of the Scientific Advisory Board of Rational Vaccines, Inc., which has licensed U.S. patents 77856605 and 8802109 for the 0ΔNLS vaccine. No other author has any competing financial interests.

Declaration of interests

The authors declare that they have no known competing financial interests or personal relationships that could have appeared to influence the work reported in this paper.

Keywords

Herpes simplex virus type 1; cornea; vaccine; neovascularization; neonatal Fc receptor

1. Introduction

Herpes simplex virus 1 (HSV-1)[1] is a highly successful human pathogen with a seroprevalence rate greater than 50% in adults worldwide [1]. One of the prominent clinical manifestations that can result from HSV-1 infection is herpes stromal keratitis, a condition that includes corneal neovascularization and lymphangiogenesis, scarring, neurotrophic keratitis, and opacity that individually or collectively contribute to visual impairment [2–4]. This pathologic condition is thought to be driven primarily by the host immune response including neutrophil influx, macrophage, and $CD4^+$ T cell activation and the production of soluble mediators that contribute directly or indirectly to the degradation of extracellular matrix proteins and collagen lamellae [5, 6]. Collateral damage to ocular-associated tissue including the lacrimal glands has also been reported in experimental models [7, 8]. In the human patient and experimentally, steroids including dexamethasone have been shown to be quite effective in reducing pathology associated with ocular HSV-1 infection but with possible consequences to long-term effects on the immune system [9–11]. Anti-viral therapeutics and recently developed novel compounds show promise experimentally in treating ongoing infection but the application in the prevention of reactivation or primary acute infection is not evident [2].

Vaccines have long been recognized as a strategy to prevent ocular HSV-1 infection [12]. However, there are no ongoing clinical trials registered in the United States evaluating vaccines against ocular HSV-1 infection, in part, likely due to the degree of difficulty in preservation of an incredibly sensitive tissue and experimental designs that do not take into account quantifiable measurements of ocular morbidity [13]. Over the past decade experimental findings have demonstrated the efficacy of strategically designed subunit vaccines to glycoproteins or peptide epitopes of glycoproteins or tegument proteins of HSV-1 in terms of suppressing viral replication and establishment of latency, generating a robust T cell response, and reducing ocular inflammation in mice [14–18]. Likewise, other labs have used attenuated HSV-1 as vaccines to demonstrate strong protection against ocular challenge with laboratory strains or clinical isolates of HSV-1 in mice and non-human primates [19–22]. In all instances, these studies fall short of evaluating the visual axis or assessing pathology in quantifiable terms. We have previously shown an attenuated HSV-1 in which the nuclear localization signal of infected cell protein 0 (ICP0) has been deleted, HSV-1 0ΔNLS, used as a vaccine provides significant efficacy against ocular HSV-1 challenge in mice [23, 24]. The vaccine was found to be safe in mice deficient in the functional type I interferon (IFN) response but cornea pathology including robust neovascularization was noted in the surviving animals [25]. Using siRNA to target expression of the neonatal Fc receptor (FcRn) expression in the cornea, we found the

[1]HSV-1, herpes simplex virus 1; ICP0, infected cell protein 0; IFN, interferon; FcRn, neonatal Fc receptor; FcRn KO, FcRn deficient; WT, wild type; PFU, plaque forming units; pi, post infection; TG, trigeminal ganglia; BS, brain stem; CNS, central nervous system; MLN, mandibular lymph node; GC, germinal center.

efficacy of the vaccine in blocking virus replication locally was compromised suggesting a role of FcRn in HSV-1 0ΔNLS vaccine efficacy within the eye [26].

The FcRn was originally described in the transport of IgG in the gut of neonatal rodents and was later reported to be responsible for the transport of IgG across the placenta of humans [27–29]. It was also determined the FcRn is crucial for the extended half-life of IgG removing it from the lysosomal degradation pathway [30, 31]. The mammalian FcRn is expressed on epithelial cells where it can transport IgG across polarized cells providing a first-line defense against invading microbial pathogens [32, 33]. In fact, the FcRn has been described to facilitate intracellular neutralization of the PR8 influenza virus likely through blocking viral assembly [34]. Within the eye, the FcRn is found associated with retina and iris blood vessels as well as the corneal epithelium and endothelial layer [35]. Previously, we reported the FcRn within the cornea is up-regulated in response to trauma or HSV-1 infection co-localizing with HSV-1 antigen in corneal epithelial cells [26]. The present study was undertaken to pursue the hypothesized role of corneal FcRn expression as a conduit of anti-HSV-1 IgG to suppress virus replication and viral-mediated cornea pathology comparing wild type to FcRn deficient (FcRn KO) mice following immunization with the HSV-1 0ΔNLS vaccine.

2. Materials and method

2.1 Mice

C57BL/6 (wild type, WT) and FcRn KO (B6.Cg-*Fcgrt*^{tm1Dcr} Tg(CAG-FCGRT)276Dcr/DcrJ) [36] male and female mice (6–8 weeks old) were obtained from The Jackson Laboratory (Bar Harbor, ME) and housed in a specific pathogen-free vivarium at the Dean A. McGee Eye Institute and University of Oklahoma Health Sciences Center. Animals were handled in accordance with the National Institutes of Health's *Guide for the Care and Use of Laboratory Animals* with all procedures approved by the University of Oklahoma Health Sciences Center Institutional Animal Care and Use Committee (Protocol #19-060-ACHIX). Mice were anesthetized for all procedures using an intraperitoneal injection of xylazine (6.6 mg/kg) and ketamine (100 mg/kg). For terminal experiments, animals were anesthetized and euthanized by exsanguination via intracardiac perfusion with 10–15 ml of PBS.

2.2 Vaccination and ocular infection

WT and FcRn KO mice were immunized with 1×10^4 plaque forming units (PFU) of the live attenuated HSV-1 0ΔNLS or vehicle (PBS) in a two-dose prime-boost regimen in the footpad and flank, respectively as previously described [23]. Animals were boosted 21 days following primary immunization and subsequently challenged with 1×10^4 PFU HSV-1 McKrae/cornea 30 days post-boost. Specifically, 3 μl of RPMI-1640 containing 10% fetal bovine serum and virus were applied to the scarified cornea of each eye of anesthetized mice. Scarification was conducted on anesthetized animals immediately before infection by using a 25 gauge needle and subjecting the cornea to partial epithelial debridement. Mice were monitored for survival out to day 30 post infection (pi) or euthanized at the indicated time point.

2.3 Serological assays

Peripheral blood was collected from the facial vein of anesthetized mice 30 days post-boost immediately before infection. The serum was obtained by fractionating the blood using Microtainer serum separation tubes (Becton Dickinson, Franklin Lakes, NJ). The collected sera was evaluated for virus-neutralizing antibody titers in the presence of guinea pig complement (Rockland, Limerick, PA) using confluent Vero cell (American Type Culture Collection, Manassas, VA) as described [23]. Anti-HSV-1 IgG2b in sera was determined by ELISA using immobilized HSV-1 virions on EIA 96-well plates (Costar, Cambridge, MA) as previously described [37].

2.4 Viral titer

Following ocular HSV-1 infection, the corneas of vaccinated mice were swabbed with cotton-tipped applicators for infectious virus in the tear film, and tissues were collected and assayed for viral content by standard plaque assay using Vero cell monolayers [23].

2.5 Ocular pathology

To measure opacity, the whole eye was excised from exsanguinated mice at the indicated time point pi, and the cornea of each eye was separated from the remainder of the tissue at the limbus interface and placed in the bottom and center of the well of a 96-well, U-bottom plate containing 50 μl of PBS. The tissue was assayed for absorbance at 500 nm using a FLUOstar Omega plate reader (BMG Labtech, Offenburg, Germany) as previously described [38]. Immediately after analysis of corneal opacity the tissue was fixed in a 4% solution of paraformaldehyde (Sigma-Aldrich, St. Louis, MO) for 30 min, and washed in PBS containing 1% Triton X-100 (Sigma-Aldrich). The corneas were blocked overnight in 10% donkey serum (Abcam, Boston, MA) and labeled for blood and lymphatic vessels as previously described [39]. Images were acquired using an Olympus FV1200 scanning confocal microscope in sequential scanning channel mode (Center Valley, PA). The total area positive for blood and lymphatic vessels per field of view (4 quadrants/cornea) was quantified using Metamorph software (Molecular Devices Inc., San Jose, CA).

2.6 Flow cytometry

Mandibular lymph nodes were macerated over 40-μm mesh cell strainer (Midsci, Valley Park, MO) into single-cell suspensions. Cells were enumerated and 1×10^6 cells/100 μl PBS containing 2% FBS were blocked with anti-CD16/32 (eBioscience, San Diego, CA), labeled with a combination of 1 μl each of CD45 PerCP-Cy5.5 (Biolegend, San Diego, CA), CD19 APC, CD3e, CD4 APC-Cy7, CD8a PE or APC-Cy7, IgM FITC, IgD PE-Cy7, CD44 APC, and/or CD62L FITC (all from Thermo Fischer Scientific) diluted in 1% BSA in 1X PBS for 30 minutes. In the case of tetramer staining, cells were labeled with a combination of CD3 PE-Cy7, CD8-APC-Cy7, gB (SSIEFARL)-PE or ICP6 (QTFDFGRL)-Alexafluor488 (NIH Tetramer Core Facility, Atlanta, GA). Cells were then washed twice by adding 1 ml of 2% FBS in 1X PBS, centrifuging for 5 minutes at 300 × g, and decanting supernatant. Cells were then fixed in 1 ml of 1% paraformaldehyde overnight and resuspended in 1 ml of 2% FBS in 1X PBS to be analyzed on a MacsQuant 196 flow cytometer (Miltenyi Biotech). Gating strategies were identical to those previously described [40] except those included in

this study, incubated on ice in the dark for 20–30 min, and washed in PBS containing 2% FBS. Samples were analyzed using FlowJo software (Ashland, OR).

2.7 Statistics

Statistical analysis of data was performed using Prism 8 software (version 8.0; GraphPad Software, La Jolla, CA). Data were analyzed between groups using the indicated analysis for statistical significance if the comparison yielded a p-value < 0.05.

3. Results

3.1 The absence of the FcRn has no significant impact on mortality even with a significant reduction in neutralizing antibody titers

Survival has often been used to establish the effectiveness of vaccines against life-threatening pathogens including HSV-1 in animal models [20–22]. In order to investigate the role of the FcRn in HSV-1 0ΔNLS vaccine efficacy, WT and FcRn KO mice were immunized with HSV-1 0ΔNLS or vehicle and subsequently challenged with HSV-1 McKrae (Fig. 1A). Vehicle-immunized FcRn KO mice showed significant mortality following ocular HSV-1 infection with a survival rate of 12.5% (1/8) compared to vehicle-immunized WT mice with a survival rate of 50% (4/8) (Fig. 1B). By comparison, HSV-1 0ΔNLS immunized WT and FcRn KO mice showed 100% survival (8/8) following ocular HSV-1 challenge (Fig. 1B).

Antibody neutralizing titers are often instrumental in the prophylactic efficacy of vaccines against infectious pathogens including HSV-1 as we previously reported using the HSV-1 0ΔNLS vaccine [23]. To determine whether neutralizing antibody titers were altered comparing immunized WT to FcRn KO mice, sera was obtained from vaccinated mice prior to ocular HSV-1 challenge and assessed for neutralization capacity and reactivity to HSV-1 antigen. Even though HSV-1 0ΔNLS vaccinated FcRn KO mice survived ocular HSV-1 challenge, the neutralization antibody titer of these animals was significantly below that of the HSV-1 0ΔNLS vaccinated WT animals (Fig. 1C). In addition, IgG2b reactivity in the sera of the HSV-1 0ΔNLS vaccinated FcRn KO mice was well below that of the WT counterparts (Fig. 1D). No other immunoglobulin isotype evaluated including IgA, IgM, IgG1, or IgG2a was found to interact with HSV-1 antigen at the level of the IgG2b isotype at the dilutions reported (data not shown).

3.2 The absence of the FcRn does not affect the outcome of HSV-1 replication, spread, or shedding in HSV-1 0ΔNLS vaccinated mice

We previously reported a 50% reduction in FcRn expression by siRNA targeting led to a loss in HSV-1 0ΔNLS vaccine efficacy as measured by viral load in the cornea 48 hr pi [26]. Therefore, we analyzed whether the absence of the FcRn in vaccinated mice significantly altered the course of viral replication compared to WT vaccinated animals. In terms of viral shedding following ocular challenge, the activity of the HSV-1 0ΔNLS vaccine was not compromised in the absence of FcRn with the lack of detectable infectious virus in the tear film by day 4 pi in both WT and FcRn KO immunized mice (Fig. 2A). Similar results were found in assessment of viral titers measured in the cornea (Fig. 2B), trigeminal ganglia (TG)

(Fig. 2C), and brain stem (BS) (Fig. 2D) of HSV-1 0ΔNLS immunized WT and FcRn KO mice at day 7 pi. In contrast, vehicle-immunized FcRn KO mice shed significantly more virus than vehicle-immunized WT mice at day 4–6 pi (Fig. 2A) but both vehicle-vaccinated mice showed similar levels of infectious virus in the cornea, TG, and BS at day 7 pi and significantly more than the HSV-1 0ΔNLS vaccinated WT or FcRn KO animals (Fig. 2B–D).

HSV-1 spreads to various regions of the central nervous system (CNS) including the olfactory bulb, hippocampus, midbrain, cerebellum, and subventricular zone after ocular infection in mice [41]. In fact, the ependymal region of the subventricular zone has been associated with severe pathology correlative with encephalitis in mice and in a subpopulation of humans diagnosed with herpes simplex encephalitis [42, 43]. Since there was a significant difference in survival between HSV-1 0ΔNLS- vs vehicle-vaccinated mice, we investigated various regions of the brain to determine if viral load correlated with mortality rates. Infectious virus was undetectable in all areas of the CNS of HSV-1 0ΔNLS vaccinated WT and FcRn KO mice. HSV-1 was detected in the subventricular zone (Fig 2E) and hippocampus (Fig. 2F) of two out of five vehicle vaccinated mice evaluated but there was no significant difference between WT and FcRn KO vehicle immunized animals. However, the frequency of detection of HSV-1 in the midbrain was higher with 60–75% of vehicle-vaccinated mice possessing detectable lytic virus but no difference between vehicle-immunized WT and FcRn KO mice (Fig. 2G).

3.3 HSV-1 0ΔNLS vaccinated WT and FcRn KO mice show minimal cornea pathology post HSV-1 infection

A hallmark of severe ocular HSV-1 infection includes corneal opacity and neovascularization consisting of the genesis of blood and lymphatic vessels in the central cornea [3, 5]. To determine whether the absence of the FcRn impacted the efficacy of the HSV-1 0ΔNLS vaccine against viral-mediated tissue pathology, vehicle- and HSV-1 0ΔNLS-immunized WT and FcRn KO mice that survived acute infection were evaluated for corneal opacity and neovascularization. Both WT and FcRn KO mice immunized with the HSV-1 0ΔNLS vaccine showed minimal corneal opacity similar to baseline levels at 30 days pi (Fig. 3A). In contrast, vehicle-immunized mice displayed a significant increase in corneal opacity compared to the HSV-1 0ΔNLS vaccinated group with no difference comparing vehicle-immunized WT to FcRn KO mice at day 30 pi (Fig. 3A). Since there was only two eyes to evaluate for the vehicle-vaccinated FcRn KO mice at day 30 pi due to mortality, we assessed the opacity in vehicle-immunized mice that required euthanasia between days 7–11 pi. Vehicle-immunized FcRn KO mice showed a significant increase in corneal opacity during this time period in comparison to their WT counterparts suggesting the lack of FcRn significantly impacts on the development of tissue pathology in response to ocular HSV-1 infection (Fig. 3B). The level of opacity was similar to that observed at day 30 pi suggesting the FcRn KO mice are highly susceptible to corneal opacity with an earlier onset relative to WT animals.

We have previously reported impressive blood and lymphatic vessel growth into the central cornea by day 30 pi in WT mice [44]. Consistent with this observation, vehicle-vaccinated WT mice showed significant corneal neovascularization by day 30 pi (Fig. 3C). Although

limited in number, a similar observation was found in the vehicle-immunized FcRn KO mice (Fig 3C). In contrast, HSV-1 0ΔNLS vaccinated WT and FcRn KO mice showed little to no neovascularization at the same day 30 pi time point (Fig. 3C). The results comparing the blood (Fig. 3D) and lymphatic (Fig. 3E) vessel genesis into the cornea proper were found to be significantly reduced in the WT groups vaccinated with HSV-1 0ΔNLS compared to the vehicle-immunized group.

3.4 Draining lymph node profile in WT and FcRn vaccinated mice

The FcRn is known to contribute to the host immune response in addition to transport of IgG. Specifically, the FcRn has been described to facilitate the uptake of antigen-antibody complexes by $CD11c^+$ dendritic cells and generate an expansion of antigen-specific $CD4^+$ T cells in organized lymphoid tissue [45]. It has also been instrumental in vaginal herpes simplex virus type 2 infection via the movement of protective, anti-viral IgG, across epithelial barriers in passively immunized mice [46]. Relative to $CD8^+$ T cell activity, the FcRn has been described to be involved in cross-presentation of antigen-IgG complexes in $CD8^-CD11b^+$ dendritic cells [47]. Therefore, we investigated the adaptive immune response in the draining (mandibular) lymph node (MLN) [48] of vaccinated WT and FcRn KO mice following HSV-1 infection. Analysis of the $CD4^+$ T cell response revealed the total $CD4^+$ T cell number recovered from the MLN of the HSV-1 0ΔNLS vaccinated mice was reduced by over 2-fold compared to the vehicle-vaccinated WT mice at day 7 pi (Fig. 4A). There was also a modest reduction in the total $CD4^+$ T cell number recovered in the MLN from HSV-1 0ΔNLS-vaccinated compared to the vehicle-vaccinated FcRn KO mice but the difference did not reach significance (Fig. 4A). Analysis of $CD4^+$ central ($CD3^+CD4^+CD44^+CD62L^+$) (Fig. 4B, 4I) and effector ($CD3^+CD4^+CD44^+CD62L^-$) (Fig. 4C, 4I) memory T cells were not significantly modified in number comparing all four groups of vaccinated WT and FcRn KO mice. There were no differences comparing WT to FcRn KO vaccinated mice for any $CD4^+$ T cell phenotype evaluated (Fig. 4A–C).

In comparison to $CD4^+$ T cells, analysis of the $CD8^+$ T cell response revealed the total $CD8^+$ T cell number of the HSV-1 0ΔNLS vaccinated mice was reduced by over 3-fold compared to the vehicle-vaccinated WT mice at day 7 pi (Fig. 4D). A similar trend was also observed in the FcRn KO vaccinated animals although it did not reach significance (Fig. 4D). There was also a significant reduction in the number of $CD8^+$ central ($CD3^+CD8^+CD44^+CD62L^+$) (Fig. 4E, 4I) and effector ($CD3^+CD8^+CD44^+CD62L^-$) (Fig. 4F, 4I) memory T cells comparing the HSV-1 0ΔNLS- to vehicle-vaccinated WT mice. However, this difference was not reflected in changes in the number of HSV-1 gB- (Fig. 4G) or ICP6- (Fig. 4H) specific $CD8^+$ T cells comparing the HSV-1 0ΔNLS- to vehicle-vaccinated WT mice. There were no differences comparing WT to FcRn HSV-1 0ΔNLS-vaccinated mice for any $CD8^+$ T cell phenotype (Fig. 4D–I). This analysis included the frequency of HSV gB- and ICP6-specific $CD8^+$ T cells to the total $CD8^+$ T cell population in the draining lymph node. Specifically, the frequency of gB-specific $CD8^+$ T cells to the total $CD8^+$ T cell population for FcRn KO vehicle-, FcRn KO 0ΔNLS-, WT vehicle-, and WT 0ΔNLS-vaccinated mice was 1.24 ± 0.21, 2.17 ± 0.76, 1.25 ± 0.28, and 1.38 ± 0.26 percent respectively. Likewise, the frequency of ICP6-specific $CD8^+$ T cells to the total $CD8^+$ T cell population for FcRn KO vehicle-, FcRn KO 0ΔNLS-, WT vehicle-, and WT 0ΔNLS-vaccinated mice was 1.03 ± 0.23, 0.70 ±

0.13, 0.62 ± 0.27, and 1.16 ± 0.23 percent respectively. However, there were significantly less effector and central memory $CD8^+$ T cells comparing vehicle-immunized FcRn KO mice compared to the vehicle-vaccinated WT animals (Fig. 4E, 4F).

Since there were some notable changes in the number of T cells in the MLN of vaccinated mice post HSV-1 infection, we also investigated possible changes in the distribution of B lymphocytes in the MLN of vaccinated mice post HSV-1 infection. The total number of $CD19^+$ B lymphocytes residing in the MLN of vehicle-vaccinated WT and FcRn KO mice was substantially higher than that found in the MLN of the HSV-1 0ΔNLS-vaccinated counterparts (Fig. 5A). A similar profile was also observed in the number of germinal center (GC) B cells with significantly elevated numbers found in the MLN of vehicle-vaccinated WT and FcRn KO mice compared to the HSV-1 0ΔNLS-vaccinated mice (Fig. 5B, 5D). However, only the WT vehicle-vaccinated mice displayed an increase in isotype-switched B lymphocyte numbers compared to the HSV-1 0ΔNLS-vaccinated WT mice (Fig. 5C, 5D). No significant difference was found comparing the FcRn KO vaccinated groups although there was a trend towards an increased number of isotype-switched B lymphocytes in the vehicle-vaccinated FcRn KO mice (Fig. 5C, 5D).

4. Discussion

The FcRn is a non-polymorphic heterodimer composed of an MHC class I-related α-chain non-covalently associated with β-2 microglobulin that acts as an IgG salvage receptor extending the circulating half-life of the IgG molecule [27, 49, 50]. FcRn expression in the cornea of mice, which is up-regulated in response to HSV-1 infection, was found to be instrumental in the control of local (i.e., cornea) HSV-1 replication in HSV-1 0ΔNLS vaccinated mice within the first 48 hr pi following targeting of its expression using siRNA [26]. In the current study, the FcRn was not found to play a significant role in vaccine efficacy in FcRn KO mice immunized with the HSV-1 0ΔNLS vaccine in terms of survival, control of virus replication and spread, and virus-mediated corneal pathology including neovascularization and opacity. However, the absence of the FcRn was found to significantly reduce the antibody neutralization titer against as well as the level of reactivity to HSV-1 in 0ΔNLS vaccinated mice. This observation is likely due to the contribution of the FcRn and circulating IgG levels that are reduced in FcRn KO mice [36]. However, both WT and FcRn KO mice exhibited similar resistance to HSV-1 replication, spread, and tissue pathology compared to the vehicle-immunized control mice. Such results would suggest (a) redundant pathway(s) may be functional in the absence of the FcRn during development. Candidate molecules include the Fcγ receptor III found on B cells, monocytes/macrophages, neutrophils, dendritic cells, and other granulocytes and Fcγ receptor IV found on monocyte/macrophages and neutrophils [51], Fc receptor-like molecules [52], and tripartite motif-containing 21 (TRIM21) protein [53]. While these membrane bound and cytosolic receptors likely play a role in anti-viral defense through the action of antibody ligation, in the case of ocular HSV-1 infection, a recent report suggests TRIM21 antagonizes the host cell resistant to the pathogen by reducing IFN-β production and inhibiting signaling through the stimulator of IFN genes/interferon regulatory factor 3 [54]. Likewise, a previous study by our group showed no loss in efficacy in immunizing Fcγ receptor III mice with the 0ΔNLS

vaccine [24]. Studies will be required to determine if an overlapping role of IgG-specific receptors exists in the absence of FcRn that would explain the current findings.

A drop in the expansion of T cell populations in the MLN of HSV-1 0ΔNLS vaccinated WT and FcRn KO mice is consistent with previous reports and is attributed to less antigen exposure due to initial virus control by the action of the vaccine-induced immune response [23, 25]. It should be noted that the differences were more pronounced and significant comparing the WT HSV-1 0ΔNLS- to vehicle-vaccinated WT animals as opposed to what was observed in the FcRn KO vaccinated groups. It was anticipated there might be changes in HSV-specific $CD8^+$ T cells comparing the various vaccinated WT and FcRn KO mice as determined using the dominant gB epitope and subdominant ICP6 epitope as previously described [55]. However, there were no differences in either the number or frequency of the HSV-specific $CD8^+$ T cells in any group of vaccinated animal.

The B lymphocyte compartment displayed more robust differences in WT and FcRn KO mice immunized with the HSV-1 0ΔNLS vaccine compared to the vehicle-vaccinated control WT and FcRn mice with significant differences measuring the total B lymphocyte number as well as the number of GC B cells within the MLN. These results are somewhat surprising in that a previous study reported enhanced B lymphocyte response to antigen in FcRn-overexpressing mice [56]. We reasoned B lymphocyte expansion in the HSV-1 0ΔNLS immunized FcRn KO mice would be similar to vehicle-vaccinated groups due to the contribution of FcRn assistance in antigen presentation which would likely encompass follicular dendritic cell presentation to naive B cells in primary follicles. The observation that germinal center B cell numbers were equivalent in the MLN of HSV-1 0ΔNLS vaccinated WT and FcRn KO mice suggests FcRn is not a significant contributing factor in the development of germinal center B cells following HSV-1 infection under these conditions. In contrast to germinal center B lymphocyte numbers, there was a substantial increase in the total number of B lymphocytes in the MLN of vehicle-vaccinated mice compared to those immunized with 0ΔNLS. We believe this change reflects the response of T lymphocytes to additional antigen available that would drive B cell expansion during the primary adaptive immune response following ocular HSV-1 infection.

The absence of FcRn did have an impact on the host response to ocular HSV-1 infection comparing vehicle-immunized animals. Specifically, the mortality rate of HSV-1-infected FcRn KO mice was higher (7/8 or 87.5%) compared to WT mice (4/8 or 50%). Likewise, viral shedding in the tear film was elevated in the vehicle-immunized FcRn KO mice compared to the WT mice during acute infection which correlated with an increase in the cornea opacity score between day 7–11 pi. It was also noted the absolute number of central memory $CD8^+$ T cells residing in the MLN of FcRn KO mice was significantly reduced compared to that found in the WT mice at 7 day pi. These changes in host susceptibility to HSV-1 infection in the absence of the FcRn are consistent with the role of the FcRn in cross presentation in the development of central memory $CD8^+$ T cells [47, 57]. However, it is somewhat surprising a larger difference was not observed in the $CD4^+$ T cell compartment which has been found to be influenced by FcRn-driven $CD4^+$ T cell expansion to antigen [45].

A major caveat to the current study is the lack of functional measurements of effector T cells or other characteristics attributable to antibody that may have contributed to the efficacy of the HSV-1 0ΔNLS vaccine in the FcRn KO mice. In terms of antibody, the Fcγ receptor has a role in phagocytosis, cytokine and chemokine production, changes in B and T lymphocyte responses and antibody-dependent cellular cytotoxicity [58], the latter of which reportedly is central to the efficacy of one vaccine candidate against ocular HSV-1 infection [21]. We have previously found the absence of neutralizing antibody to HSV-1 in HSV-1 0ΔNLS-vaccinated mice still provides a powerful influence on HSV-1 surveillance through the activation of HSV-1 specific $CD8^+$ T cells [59]. While the original observation using the HSV-1 0ΔNLS vaccine resided with the correlation of protection being antibody, it is now evident additional pathways that do not rely on FcRn expression or neutralizing antibody can provide sufficient protection in the 0ΔNLS-vaccinated host to control virus infection, replication, spread, and pathology. Candidate pathways would most likely include the type I IFN and STING-dependent pathways and downstream effector molecules including RNAse L which have been found to be critical to host defense against ocular HSV-1 challenge [60].

Acknowledgements

This work was supported by NIH R01 AI053108, NEI core grant P30 EY021725, and an unrestricted grant from Research to Prevent Blindness. We thank the staff of the Dean McGee Eye Institute animal facility for their efforts in maintaining and monitoring our mice.

References

[1]. Farooq AV, Shukla D. Herpes simplex epithelial and stromal keratitis: an epidemiologic update. Surv Ophthalmol. 2012;57:448–62. [PubMed: 22542912]

[2]. Koujah L, Suryawanshi RK, Shukla D. Pathological processes activated by herpes simplex virus-1 (HSV-1) infection in the cornea. Cellular and molecular life sciences : CMLS. 2019;76:405–19. [PubMed: 30327839]

[3]. Bryant-Hudson K, Conrady CD, Carr DJ. Type I interferon and lymphangiogenesis in the HSV-1 infected cornea - are they beneficial to the host? Prog Retin Eye Res. 2013;36:281–91. [PubMed: 23876483]

[4]. Chucair-Elliott AJ, Zheng M, Carr DJ. Degeneration and regeneration of corneal nerves in response to HSV-1 infection. Investigative ophthalmology & visual science. 2015;56:1097–107. [PubMed: 25587055]

[5]. Rowe AM, St Leger AJ, Jeon S, Dhaliwal DK, Knickelbein JE, Hendricks RL. Herpes keratitis. Prog Retin Eye Res. 2013;32:88–101. [PubMed: 22944008]

[6]. Gimenez F, Suryawanshi A, Rouse BT. Pathogenesis of herpes stromal keratitis--a focus on corneal neovascularization. Prog Retin Eye Res. 2013;33:1–9. [PubMed: 22892644]

[7]. Rao P, McKown RL, Laurie GW, Suvas S. Development of lacrimal gland inflammation in the mouse model of herpes stromal keratitis. Experimental eye research. 2019;184:101–6. [PubMed: 31009613]

[8]. Montgomery ML, Callegan MC, Fuller KK, Carr DJJ. Ocular Glands Become Infected Secondarily to Infectious Keratitis and Play a Role in Corneal Resistance to Infection. Journal of virology. 2019;93.

[9]. Wilhelmus KR, Gee L, Hauck WW, Kurinij N, Dawson CR, Jones DB, et al. Herpetic Eye Disease Study: A Controlled Trial of Topical Corticosteroids for Herpes Simplex Stromal Keratitis. Ophthalmology. 2020;127:S5–s18. [PubMed: 32200827]

[10]. Chucair-Elliott AJ, Carr MM, Carr DJJ. Long-term consequences of topical dexamethasone treatment during acute corneal HSV-1 infection on the immune system. Journal of leukocyte biology. 2017;101:1253–61. [PubMed: 28115476]

[11]. Chucair-Elliott AJ, Jinkins J, Carr MM, Carr DJ. IL-6 Contributes to Corneal Nerve Degeneration after Herpes Simplex Virus Type I Infection. The American journal of pathology. 2016;186:2665–78. [PubMed: 27497323]

[12]. Metcalf JF, Whitley RJ. Protective immunity against herpetic ocular disease in an outbred mouse model. Current eye research. 1987;6:167–71. [PubMed: 3030641]

[13]. Royer DJ, Cohen A, Carr D. The Current State of Vaccine Development for Ocular HSV-1 Infection. Expert review of ophthalmology. 2015;10:113–26. [PubMed: 25983856]

[14]. Chentoufi AA, Dasgupta G, Christensen ND, Hu J, Choudhury ZS, Azeem A, et al. A novel HLA (HLA-A*0201) transgenic rabbit model for preclinical evaluation of human CD8+ T cell epitope-based vaccines against ocular herpes. Journal of immunology (Baltimore, Md : 1950). 2010;184:2561–71.

[15]. Hu K, Dou J, Yu F, He X, Yuan X, Wang Y, et al. An ocular mucosal administration of nanoparticles containing DNA vaccine pRSC-gD-IL-21 confers protection against mucosal challenge with herpes simplex virus type 1 in mice. Vaccine. 2011;29:1455–62. [PubMed: 21185849]

[16]. Dervillez X, Qureshi H, Chentoufi AA, Khan AA, Kritzer E, Yu DC, et al. Asymptomatic HLA-A*02:01-restricted epitopes from herpes simplex virus glycoprotein B preferentially recall polyfunctional CD8+ T cells from seropositive asymptomatic individuals and protect HLA transgenic mice against ocular herpes. Journal of immunology (Baltimore, Md : 1950). 2013;191:5124–38.

[17]. Srivastava R, Khan AA, Spencer D, Vahed H, Lopes PP, Thai NT, et al. HLA-A02:01-restricted epitopes identified from the herpes simplex virus tegument protein VP11/12 preferentially recall polyfunctional effector memory CD8+ T cells from seropositive asymptomatic individuals and protect humanized HLA-A*02:01 transgenic mice against ocular herpes. Journal of immunology (Baltimore, Md : 1950). 2015;194:2232–48.

[18]. Srivastava R, Khan AA, Garg S, Syed SA, Furness JN, Vahed H, et al. Human Asymptomatic Epitopes Identified from the Herpes Simplex Virus Tegument Protein VP13/14 (UL47) Preferentially Recall Polyfunctional Effector Memory CD44high CD62Llow CD8+ TEM Cells and Protect Humanized HLA-A*02:01 Transgenic Mice against Ocular Herpesvirus Infection. Journal of virology. 2017;91.

[19]. Davido DJ, Tu EM, Wang H, Korom M, Gazquez Casals A, Reddy PJ, et al. Attenuated Herpes Simplex Virus 1 (HSV-1) Expressing a Mutant Form of ICP6 Stimulates a Strong Immune Response That Protects Mice against HSV-1-Induced Corneal Disease. Journal of virology. 2018;92.

[20]. Naidu SK, Nabi R, Cheemarla NR, Stanfield BA, Rider PJ, Jambunathan N, et al. Intramuscular vaccination of mice with the human herpes simplex virus type-1(HSV-1) VC2 vaccine, but not its parental strain HSV-1(F) confers full protection against lethal ocular HSV-1 (McKrae) pathogenesis. PloS one. 2020;15:e0228252. [PubMed: 32027675]

[21]. Ramsey NLM, Visciano M, Hunte R, Loh LN, Burn Aschner C, Jacobs WR Jr., et al. A Single-Cycle Glycoprotein D Deletion Viral Vaccine Candidate, ΔgD-2, Elicits Polyfunctional Antibodies That Protect against Ocular Herpes Simplex Virus. Journal of virology. 2020;94.

[22]. Xu X, Feng X, Wang L, Yi T, Zheng L, Jiang G, et al. A HSV1 mutant leads to an attenuated phenotype and induces immunity with a protective effect. PLoS pathogens. 2020;16:e1008703. [PubMed: 32776994]

[23]. Royer DJ, Gurung HR, Jinkins JK, Geltz JJ, Wu JL, Halford WP, et al. A Highly Efficacious Herpes Simplex Virus 1 Vaccine Blocks Viral Pathogenesis and Prevents Corneal Immunopathology via Humoral Immunity. Journal of virology. 2016;90:5514–29. [PubMed: 27030264]

[24]. Royer DJ, Hendrix JF, Larabee CM, Reagan AM, Sjoelund VH, Robertson DM, et al. Vaccine-induced antibodies target sequestered viral antigens to prevent ocular HSV-1 pathogenesis, preserve vision, and preempt productive neuronal infection. Mucosal immunology. 2019;12:827–39. [PubMed: 30670763]

[25]. Royer DJ, Carr MM, Chucair-Elliott AJ, Halford WP, Carr DJ. Impact of Type I Interferon on the Safety and Immunogenicity of an Experimental Live-Attenuated Herpes Simplex Virus 1 Vaccine in Mice. Journal of virology. 2017;91.

[26]. Royer DJ, Carr MM, Gurung HR, Halford WP, Carr DJJ. The Neonatal Fc Receptor and Complement Fixation Facilitate Prophylactic Vaccine-Mediated Humoral Protection against Viral Infection in the Ocular Mucosa. Journal of immunology (Baltimore, Md : 1950). 2017;199:1898–911.

[27]. Simister NE, Mostov KE. An Fc receptor structurally related to MHC class I antigens. Nature. 1989;337:184–7. [PubMed: 2911353]

[28]. Simister NE, Story CM, Chen HL, Hunt JS. An IgG-transporting Fc receptor expressed in the syncytiotrophoblast of human placenta. Eur J Immunol. 1996;26:1527–31. [PubMed: 8766556]

[29]. Leach JL, Sedmak DD, Osborne JM, Rahill B, Lairmore MD, Anderson CL. Isolation from human placenta of the IgG transporter, FcRn, and localization to the syncytiotrophoblast: implications for maternal-fetal antibody transport. Journal of immunology (Baltimore, Md : 1950). 1996;157:3317–22.

[30]. Israel EJ, Wilsker DF, Hayes KC, Schoenfeld D, Simister NE. Increased clearance of IgG in mice that lack beta 2-microglobulin: possible protective role of FcRn. Immunology. 1996;89:573–8. [PubMed: 9014824]

[31]. Junghans RP, Anderson CL. The protection receptor for IgG catabolism is the beta2-microglobulin-containing neonatal intestinal transport receptor. Proceedings of the National Academy of Sciences of the United States of America. 1996;93:5512–6. [PubMed: 8643606]

[32]. Spiekermann GM, Finn PW, Ward ES, Dumont J, Dickinson BL, Blumberg RS, et al. Receptor-mediated immunoglobulin G transport across mucosal barriers in adult life: functional expression of FcRn in the mammalian lung. The Journal of experimental medicine. 2002;196:303–10. [PubMed: 12163559]

[33]. Horton RE, Vidarsson G. Antibodies and their receptors: different potential roles in mucosal defense. Front Immunol. 2013;4:200. [PubMed: 23882268]

[34]. Bai Y, Ye L, Tesar DB, Song H, Zhao D, Björkman PJ, et al. Intracellular neutralization of viral infection in polarized epithelial cells by neonatal Fc receptor (FcRn)-mediated IgG transport. Proceedings of the National Academy of Sciences. 2011;108:18406–11.

[35]. Kim H, Fariss RN, Zhang C, Robinson SB, Thill M, Csaky KG. Mapping of the neonatal Fc receptor in the rodent eye. Investigative ophthalmology & visual science. 2008;49:2025–9. [PubMed: 18436836]

[36]. Petkova SB, Akilesh S, Sproule TJ, Christianson GJ, Al Khabbaz H, Brown AC, et al. Enhanced half-life of genetically engineered human IgG1 antibodies in a humanized FcRn mouse model: potential application in humorally mediated autoimmune disease. Int Immunol. 2006;18:1759–69. [PubMed: 17077181]

[37]. Halford WP, Gebhardt BM, Carr DJ. Acyclovir blocks cytokine gene expression in trigeminal ganglia latently infected with herpes simplex virus type 1. Virology. 1997;238:53–63. [PubMed: 9375008]

[38]. Filiberti A, Gmyrek GB, Montgomery ML, Sallack R, Carr DJJ. Loss of Osteopontin Expression Reduces HSV-1-Induced Corneal Opacity. Investigative ophthalmology & visual science. 2020;61:24.

[39]. Wuest TR, Carr DJ. VEGF-A expression by HSV-1-infected cells drives corneal lymphangiogenesis. The Journal of experimental medicine. 2010;207:101–15. [PubMed: 20026662]

[40]. Carr DJJ, Gmyrek GB, Filiberti A, Berube AN, Browne WP, Gudgel BM, et al. Distinguishing Features of High- and Low-Dose Vaccine against Ocular HSV-1 Infection Correlates with Recognition of Specific HSV-1-Encoded Proteins. Immunohorizons. 2020;4:608–26. [PubMed: 33037098]

[41]. Menendez CM, Jinkins JK, Carr DJ. Resident T Cells Are Unable To Control Herpes Simplex Virus-1 Activity in the Brain Ependymal Region during Latency. Journal of immunology (Baltimore, Md : 1950). 2016;197:1262–75.

[42]. Conrady CD, Zheng M, van Rooijen N, Drevets DA, Royer D, Alleman A, et al. Microglia and a functional type I IFN pathway are required to counter HSV-1-driven brain lateral ventricle enlargement and encephalitis. Journal of immunology (Baltimore, Md : 1950). 2013;190:2807–17.

[43]. Kroll CM, Zheng M, Carr DJ. Enhanced resistance of CXCR3 deficient mice to ocular HSV-1 infection is due to control of replication in the brain ependyma. Journal of neuroimmunology. 2014;276:219–23. [PubMed: 25139013]

[44]. Gurung HR, Carr MM, Bryant K, Chucair-Elliott AJ, Carr DJ. Fibroblast growth factor-2 drives and maintains progressive corneal neovascularization following HSV-1 infection. Mucosal immunology. 2018;11:172–85. [PubMed: 28378806]

[45]. Yoshida M, Claypool SM, Wagner JS, Mizoguchi E, Mizoguchi A, Roopenian DC, et al. Human neonatal Fc receptor mediates transport of IgG into luminal secretions for delivery of antigens to mucosal dendritic cells. Immunity. 2004;20:769–83. [PubMed: 15189741]

[46]. Li Z, Palaniyandi S, Zeng R, Tuo W, Roopenian DC, Zhu X. Transfer of IgG in the female genital tract by MHC class I-related neonatal Fc receptor (FcRn) confers protective immunity to vaginal infection. Proceedings of the National Academy of Sciences of the United States of America. 2011;108:4388–93. [PubMed: 21368166]

[47]. Baker K, Qiao SW, Kuo TT, Aveson VG, Platzer B, Andersen JT, et al. Neonatal Fc receptor for IgG (FcRn) regulates cross-presentation of IgG immune complexes by CD8-CD11b+ dendritic cells. Proceedings of the National Academy of Sciences of the United States of America. 2011;108:9927–32. [PubMed: 21628593]

[48]. Gurung HR, Carr MM, Carr DJ. Cornea lymphatics drive the CD8(+) T-cell response to herpes simplex virus-1. Immunology and cell biology. 2017;95:87–98. [PubMed: 27577867]

[49]. Martin WL, Bjorkman PJ. Characterization of the 2:1 complex between the class I MHC-related Fc receptor and its Fc ligand in solution. Biochemistry. 1999;38:12639–47. [PubMed: 10504233]

[50]. Prabhat P, Gan Z, Chao J, Ram S, Vaccaro C, Gibbons S, et al. Elucidation of intracellular recycling pathways leading to exocytosis of the Fc receptor, FcRn, by using multifocal plane microscopy. Proceedings of the National Academy of Sciences of the United States of America. 2007;104:5889–94. [PubMed: 17384151]

[51]. Bruhns P Properties of mouse and human IgG receptors and their contribution to disease models. Blood. 2012;119:5640–9. [PubMed: 22535666]

[52]. Li FJ, Won WJ, Becker EJ, Easlick JL, Tabengwa EM, Li R, et al. Emerging Roles for the FCRL Family Members in Lymphocyte Biology and Disease. In: Daeron M, Nimmerjahn F, editors. Fc Receptors. Cham: Springer International Publishing; 2014. p. 29–50.

[53]. Watkinson RE, McEwan WA, Tam JC, Vaysburd M, James LC. TRIM21 Promotes cGAS and RIG-I Sensing of Viral Genomes during Infection by Antibody-Opsonized Virus. PLoS pathogens. 2015;11:e1005253. [PubMed: 26506431]

[54]. Tan T, Xia L. TRIM21 Aggravates Herpes Simplex Virus Epithelial Keratitis by Attenuating STING-IRF3-Mediated Type I Interferon Signaling. Frontiers in microbiology. 2020;11:703. [PubMed: 32373102]

[55]. St Leger AJ, Peters B, Sidney J, Sette A, Hendricks RL. Defining the herpes simplex virus-specific CD8+ T cell repertoire in C57BL/6 mice. Journal of immunology (Baltimore, Md : 1950). 2011;186:3927–33.

[56]. Kacskovics I, Cervenak J, Erdei A, Goldsby RA, Butler JE. Recent advances using FcRn overexpression in transgenic animals to overcome impediments of standard antibody technologies to improve the generation of specific antibodies. MAbs. 2011;3:431–9. [PubMed: 22048692]

[57]. Garg R, Latimer L, Simko E, Gerdts V, Potter A, van Drunen Littel-van den Hurk S. Induction of mucosal immunity and protection by intranasal immunization with a respiratory syncytial virus subunit vaccine formulation. The Journal of general virology. 2014;95:301–6. [PubMed: 24136365]

[58]. Bournazos S, Ravetch JV. Fcγ Receptor Function and the Design of Vaccination Strategies. Immunity. 2017;47:224–33. [PubMed: 28813656]

[59]. Gmyrek GB, Filiberti A, Montgomery M, Chitrakar A, Royer DJ, Carr DJJ. Herpes Simplex Virus 1 (HSV-1) 0ΔNLS Live-Attenuated Vaccine Protects against Ocular HSV-1 Infection in the Absence of Neutralizing Antibody in HSV-1 gB T Cell Receptor-Specific Transgenic Mice. Journal of virology. 2020;94.

[60]. Royer DJ, Carr DJ. A STING-dependent innate-sensing pathway mediates resistance to corneal HSV-1 infection via upregulation of the antiviral effector tetherin. Mucosal immunology. 2016;9:1065–75. [PubMed: 26627457]

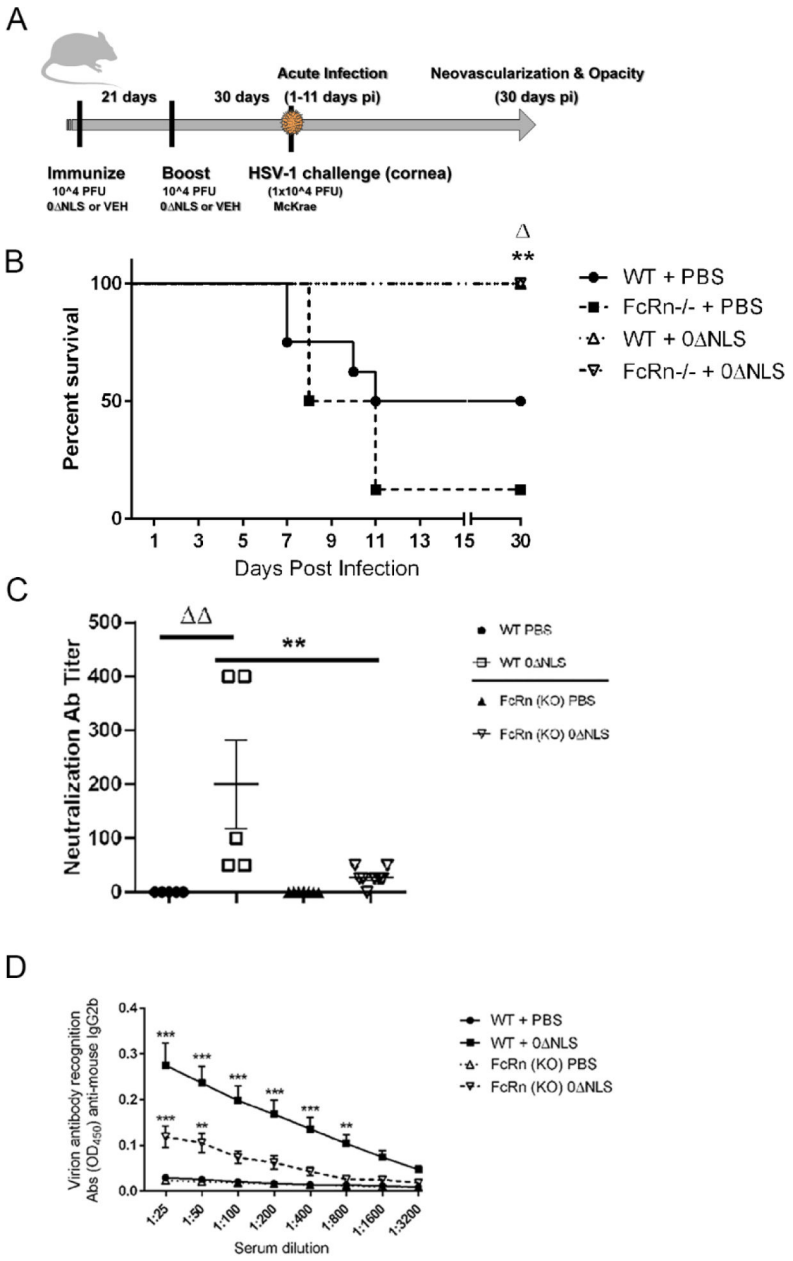

Fig. 1.

HSV-1 0ΔNLS immunized C57BL/6 (WT) and FcRn KO mice are protected from HSV-1-mediated mortality. (A) WT and FcRn KO mice (n=6–8/group) were vaccinated and boosted with HSV-1 0ΔNLS or vehicle and subsequently ocularly challenged with HSV-1 McKrae (1×10^4 PFU/cornea). At the indicated times post infection (pi), the mice were euthanized and assessed for resistance to infection and humoral immunity. (B) Mice were monitored for survival out to day 30 post infection. The results are the summary of two independent experiments; **p<.01 comparing the HSV-1 0ΔNLS vaccinated groups to the PBS immunized FcRn KO mice, $^{\Delta}$p<.05 comparing the HSV-1 0ΔNLS vaccinated groups to the PBS immunized WT mice. (C) Sera from vaccinated mice (n=10/group) was evaluated for neutralization titers. The results depict mean ± SEM, **p<.01 comparing HSV-1 0ΔNLS

vaccinated WT to FcRn KO mice and $^{\Delta\Delta}p<.01$ comparing the HSV-1 0ΔNLS vaccinated WT to the PBS-immunized WT mice as determined by ANOVA and Tukey's post hoc *t*-test. (D) IgG2b reactivity to HSV-1 antigen in sera from PBS- and HSV-1 0ΔNLS-vaccinted WT and FcRn KO mice (n=10/group). ***p<.001, **p<.01 comparing HSV-1 0ΔNLS vaccinated mice to all other groups as determined by ANOVA and Tukey's post hoc *t*-test.

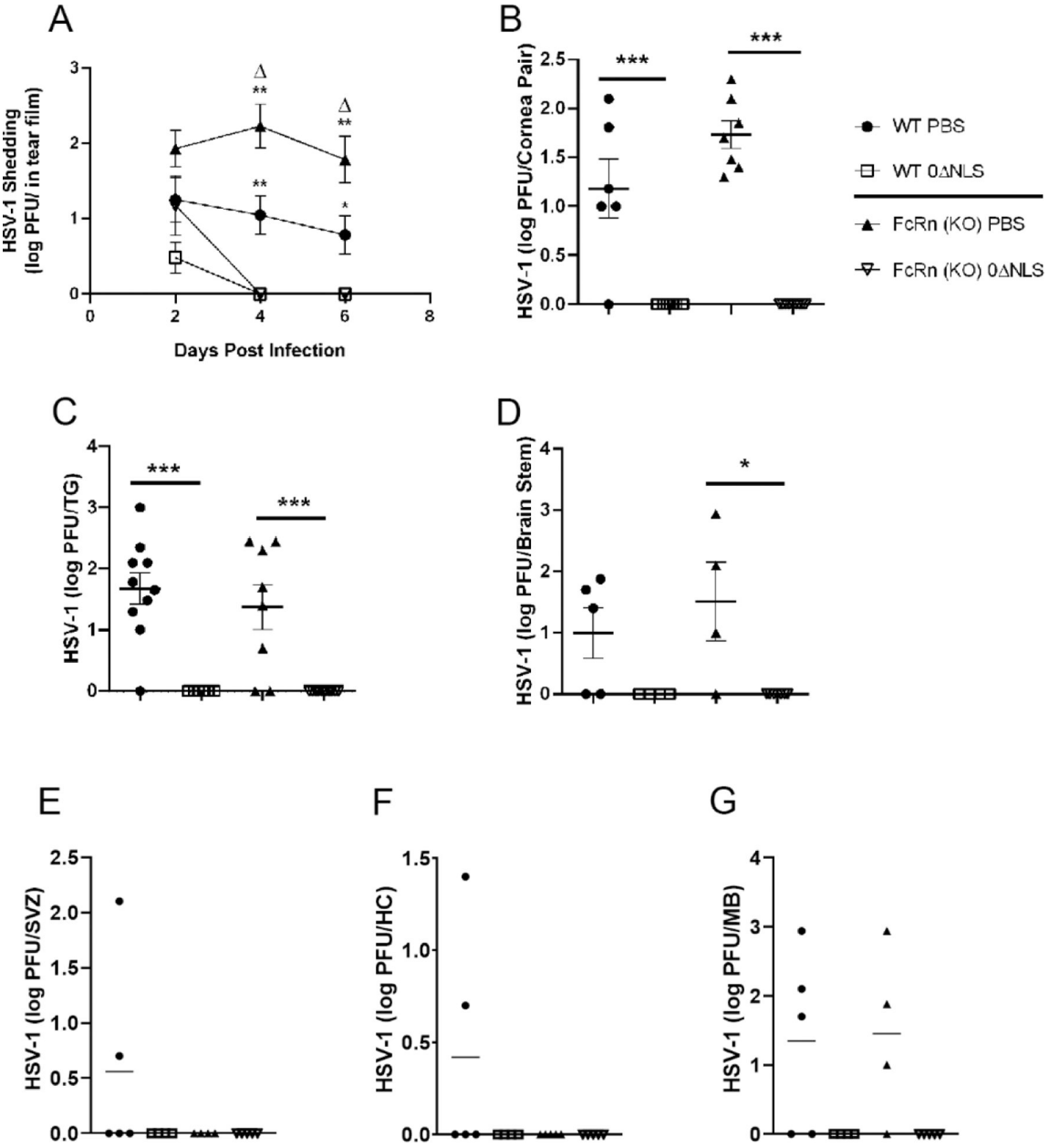

Fig. 2.

HSV-1 0ΔNLS immunized C57BL/6 (WT) and FcRn KO mice show containment of HSV-1 replication and spread. WT and FcRn KO mice (n=5–10/group) were vaccinated with HSV-1 0ΔNLS or vehicle and subsequently ocularly challenged with HSV-1 McKrae (1×10^4 PFU/cornea). The results are depicted as mean ± SEM. (A) Tear film was analyzed for viral content by plaque assay at the indicated times pi. **p<.01, *p<.05 comparing the indicated vehicle-vaccinated animals to the HSV-1 0ΔNLS immunized mice; $^{\Delta}$p<.05 comparing the vehicle-vaccinated FcRn to WT mice as determined by ANOVA and Tukey's post hoc t-test. Vaccinated mice were euthanized 7 days pi and assayed for infectious virus in the (B) cornea, (C) trigeminal ganglia (TG), (D) brain stem (BS), (E) subventricular zone (SVZ), (F) hippocampus (HC), and (G) midbrain (MB) by plaque assay. ***p<.001, *p<.05 comparing

the HSV-1 0ΔNLS immunized animals to their vehicle-vaccinated counterparts as determined by ANOVA and Tukey's post hoc *t*-test.

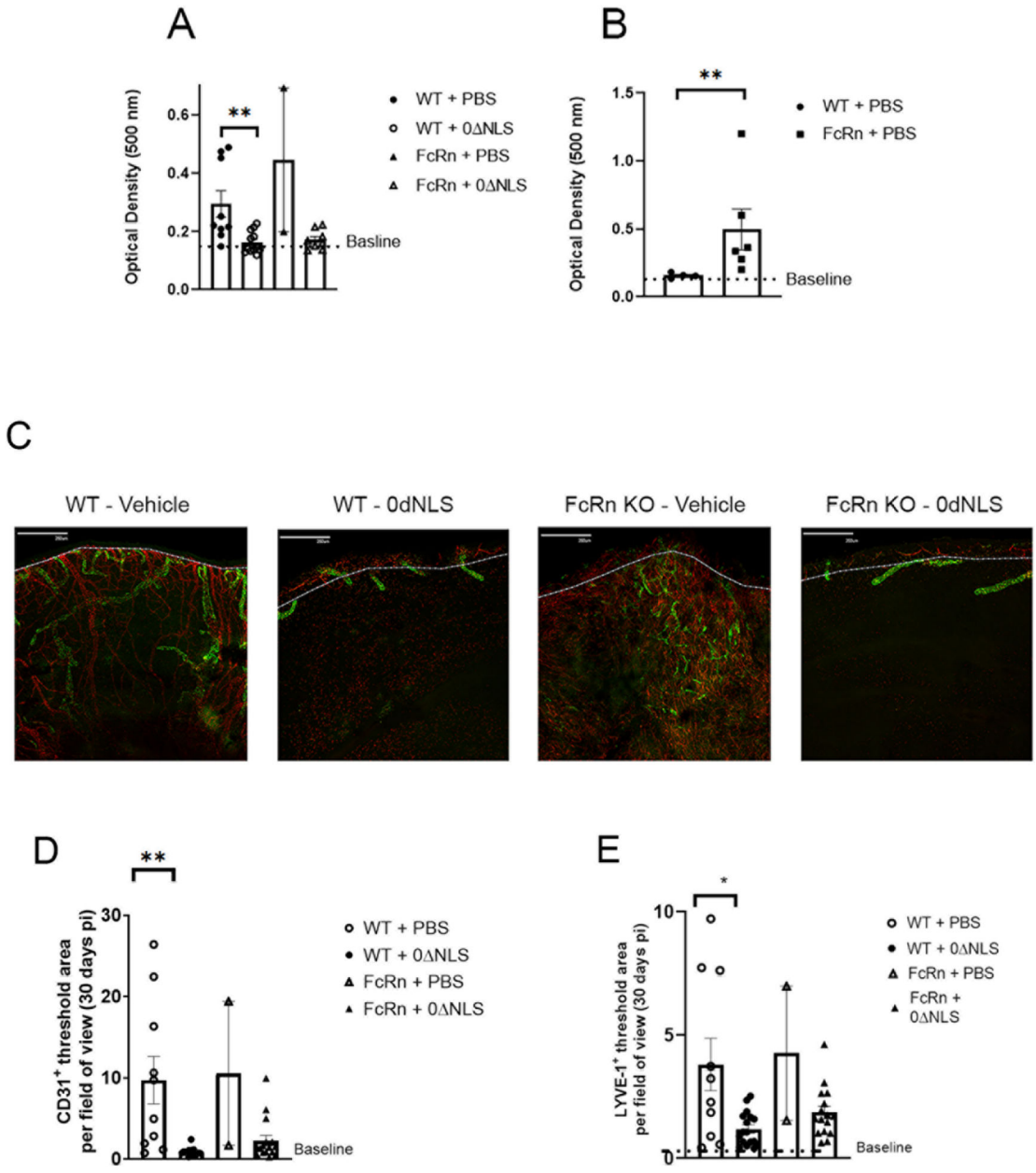

Fig. 3.

Cornea opacity and neovascularization. WT and FcRn KO mice (n=4–8/group) were vaccinated with HSV-1 0ΔNLS or vehicle and subsequently ocularly challenged with HSV-1 McKrae (1×10^4 PFU/cornea). The results are depicted as mean ± SEM (or mean ± SD for FcRn + vehicle at day 30 pi). The corneas of mice that survived infection were removed from the eyes of euthanized animals (A) day 30 pi or (B) day 7–11 pi and assessed for corneal opacity as measured by absorbance at 500 nm. **p<.01 comparing the indicated groups of vaccinated mice as determined by Mann-Whitney rank order test. (C–E)The corneas of mice that survived infection were removed from the eyes of euthanized animals and assessed for lymphatic and blood vessel genesis into the central aspect of the cornea. (C) Representative confocal images of corneas from vehicle- and HSV-1 0ΔNLS vaccinated WT

and FcRn mice at day 30 pi. Lymphatic vessels appear green and blood vessels appear red. Bar = 250 μm. Dotted line outlines the limbus margins. Summary of the threshold area of the cornea occupied by (D) $CD31^+$ blood vessels and (E) $Lyve\text{-}1^+$ lymphatic vessels for each group of mice. For panels C–E, the results are depicted as mean ± SEM (or mean ± SD for FcRn + vehicle at day 30 pi, n=2). **p<.01, *p<.05 comparing the vehicle-vaccinated to HSV-1 0ΔNLS-vaccinated groups as determined by ANOVA and Tukey's *t*-test.

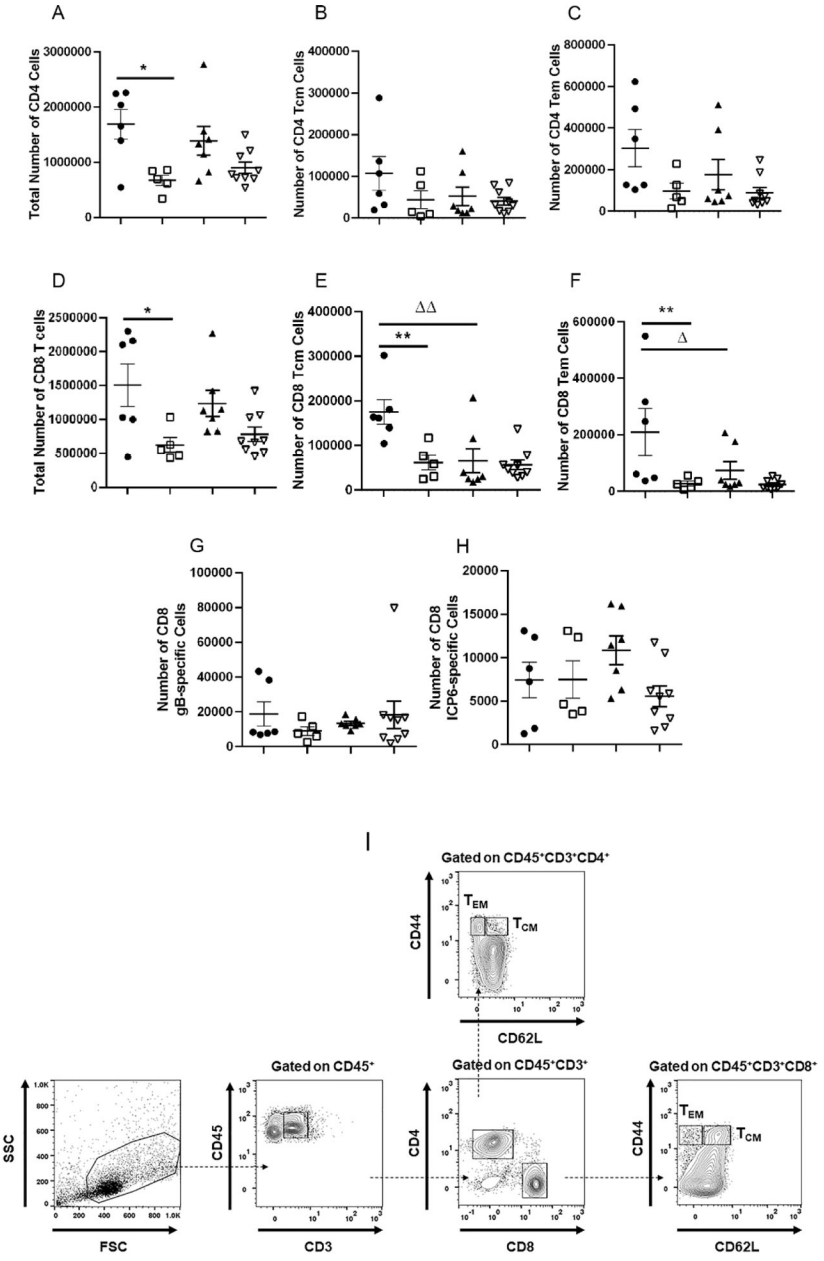

Fig. 4.

Phenotypic characterization of lymph node T cells post infection. WT and FcRn KO mice (n=5–8/group) were vaccinated with HSV-1 0ΔNLS or vehicle and subsequently ocularly challenged with HSV-1 McKrae (1×10^4 PFU/cornea). The mandibular lymph nodes were removed from exsanguinated mice at day 7 pi and examined for total $CD4^+$ T cell (A), total $CD4^+$ central memory T cell (B), total $CD4^+$ effector memory T cell (C), total $CD8^+$ T cell (D), total $CD8^+$ central memory T cell (E), total $CD8^+$ effector memory T cell (F), total HSV-1 gB-specific $CD8^+$ T cell (G), and total HSV-1 ICP6-specific $CD8^+$ T cell (H) numbers reported as mean ± SEM. (I) Gating strategy for effector ($CD3^+CD44^+CD62L^-$) and central ($CD3^+CD44^+CD62L^+$) memory $CD4^+$ and $CD8^+$ T cells. $^{\Delta\Delta}p<.01$, $^{**}p<.01$,

$^{\Delta}p<.05$, *$p<.05$ comparing the indicated groups as determined by ANOVA and Tukey's *t*-test.

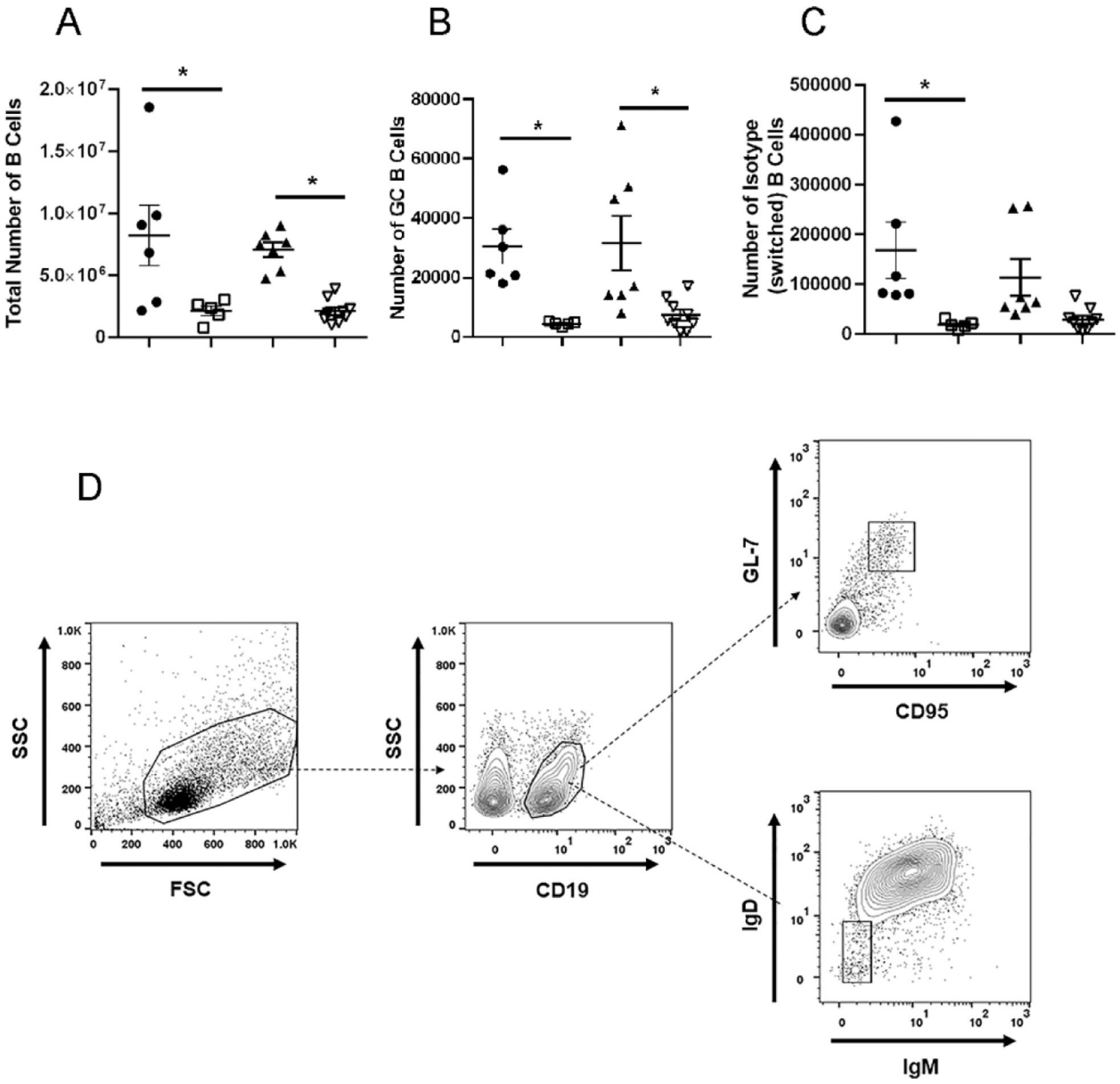

Fig. 5.

Phenotypic characterization of lymph node B cells post infection. WT and FcRn KO mice (n=5–8/group) were vaccinated with HSV-1 0ΔNLS or vehicle and subsequently ocularly challenged with HSV-1 McKrae (1×10^4 PFU/cornea). The mandibular lymph nodes were removed from exsanguinated mice at day 7 pi and examined for total B cell (A), total germinal center (GC) B cell (B), and total isotype-switch B cell (C) numbers reported as mean ± SEM. (D) Gating strategy for germinal center ($CD19^+GL\text{-}7^+CD95^+$) and isotype-switched ($IgD^-IgM^-$) B cells. *p<.05 comparing the indicated groups as determined by ANOVA and Tukey's *t*-test.